




Ultra-fast, High-Bandwidth Coherent cw THz Spectrometer for Non-destructive Testing

Lars Liebermeister¹  · Simon Nellen¹ · Robert Kohlhaas¹ · Steffen Breuer¹ · Martin Schell¹ · Björn Globisch¹

Received: 19 October 2018 / Accepted: 13 December 2018 / Published online: 9 January 2019
© The Author(s) 2019

Abstract

Continuous wave THz (cw THz) systems define the state-of-the-art in terms of spectral resolution in THz spectroscopy. Hitherto, acquisition of broadband spectra in a cw THz system was always connected with slow operation. Therefore, high update rate applications like inline process monitoring and non-destructive testing are served by time domain spectroscopy (TDS) systems. However, no fundamental restriction prevents cw THz technology from achieving faster update rates and be competitive in this field. In this paper, we present a fully fiber-coupled cw THz spectrometer. Its sweep speed is two orders of magnitude higher compared to commercial state-of-the-art systems and reaches a record performance of 24 spectra per second with a bandwidth of more than 2 THz. In the single-shot mode, the same system reaches a peak dynamic range of 67 dB and exceeds a value of 100 dB with averaging of 7 min, which is among the highest values ever reported. The frequency steps can be as low as 40 MHz. Due to the fully homodyne detection, each spectrum contains full amplitude and phase information. This demonstration of THz-spectroscopy at video-rate is an essential step towards applying cw THz systems in non-destructive, in line testing.

Keywords Continuous wave · THz · Terahertz · Spectrometer · Broadband · High update rate · NDT · Non-destructive testing

1 Introduction

Terahertz technology is pushing forward strongly into industrial applications. This is due to its extraordinary features: Contact-free determination of multi-layer thicknesses of coatings [1–3] as well as sensing for thickness variations or defects in polymers, foams, and other non-conductive materials [4]. The measurement is contact-free, non-destructive, and based on harmless, non-ionizing radiation. For real-time applications in science as well as in developments aiming for industrial use, optoelectronic time-domain THz

✉ Lars Liebermeister
lars.liebermeister@hhi.fraunhofer.de

spectroscopy dominates the field. This technology features high bandwidth and supports update rates of several hertz [5] or even kilohertz [6–8]. However, there are fundamental drawbacks regarding commercial applications: Time-domain spectroscopy not only relies on an expensive pulsed laser source, but it also requires an elaborated optical delay scheme based on free-space optics and optomechanics [5], cavity detuning [8], or a complex synchronization of two laser sources [6, 7]. All three approaches pose high demands on assembly and adjustment or require complex electronic control. In addition, such systems often have low flexibility in terms of spectral resolution. Optoelectronic continuous-wave THz-spectroscopy (cw THz) is an alternative, which is already commercially applied in gas sensing due to its high spectral resolution [9]. The advantages of cw THz systems are the unrestricted compatibility with optical fiber technology enabling fully fiber-coupled systems without any free space optics, moving parts or mechanical delay lines as well as the use of cw lasers instead of complex femtosecond pulsed lasers. Furthermore, its capabilities for non-destructive testing (NDT) have been demonstrated recently [10]. Real-world NDT applications at the production site require update rates of at least several hertz, which is a major challenge for most cw THz systems. This can be attributed to two major bottlenecks: First, a tunable laser source with a tuning range of several THz and a tuning speed of several hundred THz/s is not available off the shelf. Second, time-consuming averaging or lock-in detection is required due to compensate the intrinsically low receiver signal-to-noise ratio.

Previous demonstrations of optoelectronic cw THz systems aiming at high update rates and broadband THz-spectra (> 1 THz bandwidth), commercial and scientific, can be categorized by the technology and tuning mechanism used by the laser source. Commonly, distributed-feedback (DFB) [11] lasers, distributed Bragg reflector (DBR) lasers [12], or external-cavity diode lasers (ECDLs) [13] are used due to their off-the-shelf availability. However, none of these concepts offers high tuning speed (> 100 THz/s) and a broad tuning range ($\gg 1$ THz) at the same time. While DBR lasers provide a wide tuning range (in case mode transitions are allowed) of up to 2.6 THz [12], their thermal tuning mechanism is inherently slow. Considerably faster tuning of DFB lasers has been demonstrated by using micro heaters [14, 15]. However, with microheaters, the tuning range was limited again to 1 THz only. In addition, the acquisition rate of the demonstrated system was low due to the use of a mechanical delay. Another demonstration uses a wavelength-swept laser with high sweep rates of 1 kHz. In this case, as the noise suppression relies on time-consuming averaging, the effective acquisition time for a signal-to-noise ratio of 40 dB was about 10 s [16]. In addition, due to non-coherent detection, no phase information was obtained. With ECDLs moderate update rates of 0.3 Hz and coherent detection has been demonstrated [10, 17]. However, ECDLs are bulky and expensive due to their mechanical components. In conclusion, the acquisition of broadband cw THz spectra at fast update rates has not been demonstrated yet.

In this paper, we present a coherent cw THz spectrometer with high update rates and high bandwidth. In this system an ultrafast, widely tunable modulated-grating y-branch laser is used [18]. Based on the fast tuning rate of several tens to several hundreds of THz per second, video-rate (24 Hz) full-spectral (> 2 THz) update rates are possible. This system demonstrates the potential of cw THz spectroscopy in NDT-applications by showing a performance competitive to TDS-systems but at potentially much lower system cost and footprint.

2 Setup

In optoelectronic cw THz spectroscopy, photomixing is used to convert the beat signal of two cw lasers into THz radiation. Thereby, the difference frequency of the two lasers corresponds to the emitted THz frequency. Detuning of one of the lasers allows for acquiring broad spectra in the THz frequency range. In a homodyne configuration, the same optical beat signal is used to downconvert the incoming THz signal at the receiver. The relative phase of the optical beat signal at emitter and receiver is modulated, enabling instant phase sensitive, coherent detection [19].

In this configuration, two requirements have to be met in order to achieve high update rates with broadband spectra and high frequency resolution: First, a fast sweeping laser (several 10 THz/s tuning speed), and second, a phase modulation scheme with frequencies above 100 kHz. In our setup, we fulfill these requirements with the concept shown in Fig. 1. The fast sweeping laser is a modulated-grating Y-branch laser (MG-Y) Finisar® WaveSource™. The MG-Y uses the Vernier effect with two multi-peak reflectors to achieve wide frequency tuning, spanning the whole c-band (1526.9–1568.5 nm). The tuning mechanism is based on current injection, resulting in a typical absolute wavelength accuracy better than 100 MHz and dwell times as low as 2 μ s. The operation parameters of the MG-Y laser are specified in a look-up table allowing a deterministic operation in predefined modes with a frequency reproducibility better than 10 MHz in between sweeps. The linewidth and frequency repeatability of the laser is below 10 MHz for fixed frequency operation and the power-variation over frequency is below 1 dB. Step sizes of 20 MHz and 400 MHz are used with tuning ranges of either 200 GHz or the whole c-band. The effective tuning speed is 10 THz/s and 200 THz/s, respectively. During tuning, well-defined mode jumps occur, which are indicated by the trigger scheme and omitted in the evaluation. The resulting total duty cycle of the laser is around 70–80% including mode transitions and the reset time between subsequent sweeps.

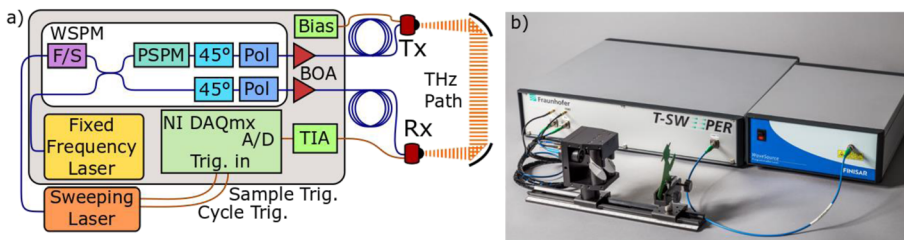


Fig. 1 **a** The optical and electrical signal path of the experimental setup employing two laser sources, a wavelength selective phase modulator (WSPM), booster optical amplifiers (BOA), transmitter bias supply (Bias), transmitter (Tx), receiver (Rx), and a THz-path established by two off-axis parabolic mirrors. The wavelength selective phase modulator assembly (white box) is based on polarization maintaining fibers and comprises a fast/slow-axis converter (F/S), a 3-dB-coupler (3 dB), a polarization selective LiNb phase modulator (PSPM), two adapter fibers with plugs rotated by 45°deg. (45°) with respect to the fast and slow axis and fiber-coupled polarizers (Po). The function principle is described elsewhere [13]. The received signal is amplified (TIA) and digitized by the data acquisition unit (NI DAQmx) together with the sample- and cycling trigger of the WaveSource™. **b** Photograph of the spectrometer. The spectrometer (left box, “T-SWEEPER”) includes all optical and electrical components listed in (a) except the sweeping laser (Finisar® WaveSource™) on the right. The photograph also shows a sensor head for reflection geometry in the front, which has been replaced by a simple 2-mirror transmission setup for the results presented here. The front of the spectrometer features the fiber input for the sweeping laser as well as the optical and electrical connectors for Tx and Rx. The spectrometer is connected to a PC via a USB connection (not shown)

A second, fixed frequency laser (ID Photonics CoBrite DX1) is used, featuring a linewidth below 100 kHz. The beating of the two laser signals is generated using an all-fiber, wavelength selective phase modulation (WSPM) scheme [20], allowing for relative phase modulation of the two output ports (WSPM in Fig. 1). The DAQ-unit drives the phase modulation with a saw-tooth voltage at 125 kHz and a peak-to-peak amplitude of 6.3 V for 2π modulation depth. The two output signals are amplified to 32 mW per output (Thorlabs BOA1004P with OptoSCI LDR1000S driver) and guided to the emitter (Tx) and the receiver (Rx), respectively. The emitter contains a waveguide-integrated PIN diode. A fiber-coupled photoconductor is used as a receiver [21]. Both emitter and receiver are commercially available at Toptica Photonics AG. The THz beam path consists of two 90° off-axis parabolic mirrors. The detector current is amplified by a Femto DLPCA-200 trans-impedance amplifier (TIA) with an amplification of 10^5 V/A and digitized using a DAQ-unit (National Instruments (NI) DAQmx USB-6366) at a rate of 2 MS/s with 16 bit vertical resolution. In order to synchronize the data acquisition with the tuning of the WaveSource™, the sample trigger indicating every valid frequency step is recorded simultaneously. An additional cycle trigger indicates the beginning of each spectrum (see Fig. 1 a).

Please note that this system contains neither moving parts nor free space optics. This gives a very robust and alignment-free system, which fits into a standard desktop case (see Fig. 1 b).

3 Acquisition Scheme

The update rate of the spectrometer is fixed to the sweep rate of the Y-branch laser, which depends on the parameters step size and tuning range. For a sweep of the full c-band in steps of 400 MHz, a continuous update rate of 24 Hz is achieved. The tuning mode used for this demonstration uses a dwell time of 2 μ s per frequency step. The data recording was performed at a sample rate of 2 MS/s; therefore, not more than four samples are acquired per dwell time. As the coherent detection scheme requires phase modulation, a lock-in like evaluation such as described below is beneficial. We found that four sampled values are insufficient to provide moderate noise suppression. However, by evaluating two subsequent frequency steps simultaneously (2 times binning, resulting in 8 samples and 4 μ s measurement time per frequency), we found a good compromise between dynamic range and frequency resolution, which is 40 MHz and 800 MHz for step sizes of 20 MHz and 400 MHz, respectively. The digitized signal of the receiver is filtered by using a bandpass centered around the modulation frequency. Subsequently, the samples of two dwell times are evaluated simultaneously by multiplication with a complex harmonic function $e^{2\pi if t_s}$ followed by summation. Here, f denotes the driving frequency of the phase modulator (125 kHz), t_s denotes absolute time when sample s is acquired and i is the imaginary unit. The complex result provides amplitude and relative phase of the detected signal in a 40 MHz or 800 MHz wide frequency window, respectively.

Due to the homodyne detection scheme, the THz amplitude as well as the relative phase angle between THz field and optical beat is recorded simultaneously. The relative phase angle ϕ_{rel} as a function of the terahertz frequency f_{THz} is given by the time-dependent contribution of the wavelength-selective phase modulator $\phi_{\text{mod}}(t_s)$, the static phase shift introduced by the path length difference (PLD) between both arms $\phi_{\text{PLD}}(f_{\text{THz}})$ and the static phase shift caused by water absorption within the THz-path $\phi_{\text{water}}(f_{\text{THz}})$

$$\phi_{\text{rel}}(f_{\text{THz}}, t_s) = \phi_{\text{mod}}(t_s) + \phi_{\text{PLD}}(f_{\text{THz}}) + \phi_{\text{water}}(f_{\text{THz}}) \quad (1)$$

The path length difference induces a linear phase shift with frequency f_{THz} of the form:

$$\phi_{\text{PLD}}(\lambda_{\text{THz}}) = 2\pi c f_{\text{THz}} (\sum_i L_{\text{Tx}_i} + \sum_i L_{\text{THz}_i} - \sum_i L_{\text{Rx}_i}) \quad (2)$$

where c is the vacuum speed of light, L_{Tx_i} indicate the optical path length elements from the beam splitter to the emitter, L_{THz_i} the THz path elements, and L_{Rx_i} the optical length from the splitter to the receiver. This model is valid for constant dispersion along the optical path. When optical fibers are used, their non-constant dispersion results in another frequency-dependent phase shift; however, this effect is very small and neglected in this argument. The additional phase shift introduced by the water absorption in the THz-path is:

$$\phi_{\text{water}}(f_{\text{THz}}) = 2\pi c f_{\text{THz}} (n_{\text{water}}(f_{\text{THz}}) - 1) \sum_i L_{\text{THz}_i} \quad (3)$$

$n_{\text{water}}(f_{\text{THz}})$ is the wavelength-dependent refractive index of humid air. Due to the lock-in like detection scheme, the phase modulation $\phi_{\text{mod}}(f_{\text{THz}}, t)$ cancels out and the measured phase shift spectrum comprises a linear term of the path length difference and the THz path including the water absorption:

$$\begin{aligned} \phi_{\text{meas}}(f_{\text{THz}}) &= \phi_{\text{PLD}}(f_{\text{THz}}) + \phi_{\text{water}}(f_{\text{THz}}) \\ &= 2\pi c f_{\text{THz}} (\sum_i L_{\text{Tx}_i} + n_{\text{water}}(f_{\text{THz}}) \sum_i L_{\text{THz}_i} - \sum_i L_{\text{Rx}_i}) \end{aligned} \quad (4)$$

Note that the phase of the laser itself has no impact on the phase measurement at the receiver, since any phase change of the laser affects both emitter and receiver equally and, therefore, cancels out. The only requirement for coherent cw THz systems is a deterministic lasing frequency to ensure a well-known THz frequency. Therefore, the Finisar® WaveSource™, with its well-defined phase changes and mode transitions is well suited for cw THz spectroscopy. The results presented in the following paragraph confirm this statement (see Fig. 3).

4 System Performance

Figure 2 a shows THz-spectra acquired with a fast sweep across the whole c-band. Using a step size of 400 MHz, THz spectra up to 3.5 THz are recorded at a rate of 24 Hz. Note that the effective bandwidth increases with averaging time. For a single-shot measurement (orange), the effective bandwidth is about 2 THz, after less than 5 s of averaging (blue), the effective bandwidth reaches 2.8 THz. With averaging of 7 min (green), the effective bandwidth is well above 3.5 THz. The peak dynamic range is 65 dB for a single-shot measurement. Note, that this value is reached by a total measurement time per frequency of not more than 4 μs . By averaging, the peak dynamic range exceeds 90 dB in less than 1 min and saturates above 100 dB after about 7 min (corresponding to 10,000 spectra). Note that this value is among the highest values of signal-to-noise ratio of any coherent cw terahertz system reported so far. This value is reached with a the record integrated measurement time per frequency of only 40 ms, 5 times lower than reported before [20]. The peak dynamic range is shown as a function of the averaging time in Fig. 2 b. An increase in averaging time by a factor of ten fits well to a gain in dynamic range of 10 dB (indicated by the gray line). This trend holds until around 7-min averaging time, which underlines the extraordinary stability of the system. The saturation of the dynamic range can be explained by non-stochastic background emerging from systematic

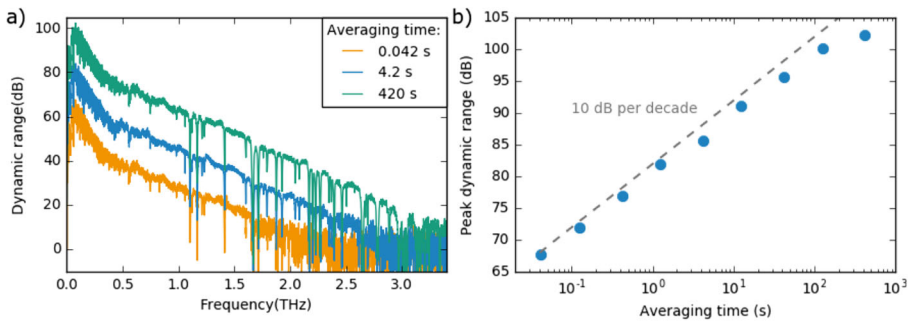


Fig. 2 **a** THz spectra obtained at a continuous update rate of 24 Hz showing single shot (acquisition time 0.042 s), an average of 100 spectra and an average of 10,000 spectra, taking 4.2 s and about 7 min, respectively. The spectra are obtained with 400 MHz step size with a data binning of two steps (spectral resolution is 800 MHz). The single-shot measurement reveals a peak dynamic range (DR) of more than 65 dB around 100 GHz, 28 dB at 1 THz and 9 dB at 2 THz. By averaging 4.2 s (420 s), the DR rises to more than 93 dB (102 dB) at 100 GHz, 47 dB (65 dB) at 1 THz, 25 dB (42 dB) at 2 THz and 0 dB (20 dB) at 2.9 THz. Note, that the signal at 3.5 THz is significantly above noise level. **b** Power peak dynamic range as a function of averaging time. The dynamic range is obtained as peak amplitude divided by the mean value obtained for frequencies from 4.35 to 4.75 THz, which is well above the emitter’s bandwidth. The averaging is performed using complex values, averaging amplitude and phase data simultaneously. The dashed gray line indicates a slope of 10 dB per decade

errors such as crosstalk of the trigger to the detector signal. Averaging is performed on the complex spectral data including phase and amplitude. This shows that the phase values in subsequent runs are fully reproducible as well. The unwrapped phase of one spectrum (7-min averaging) is plotted in Fig. 3. The linear increase of the accumulated phase with frequency indicates a path length mismatch of the emitter and receiver path.

In addition to the broad spectral tuning mode with 4.7-THz bandwidth, the Finisar® WaveSource™ can be set to a 300-GHz wide sweep mode. This mode can be used to perform spectroscopy tasks at high update rates up to 120 Hz with a spectral resolution of 800 MHz. The spectral resolution can be improved down to 40 MHz at a reduced update rate of 10 Hz. In analogy to the broad THz spectra, averaging increases the dynamic range. This mode of operation is of special relevance for spectroscopic applications. Figure 4 a and b shows atmospheric water absorption lines around 1.1 THz and 1.7 THz, respectively.

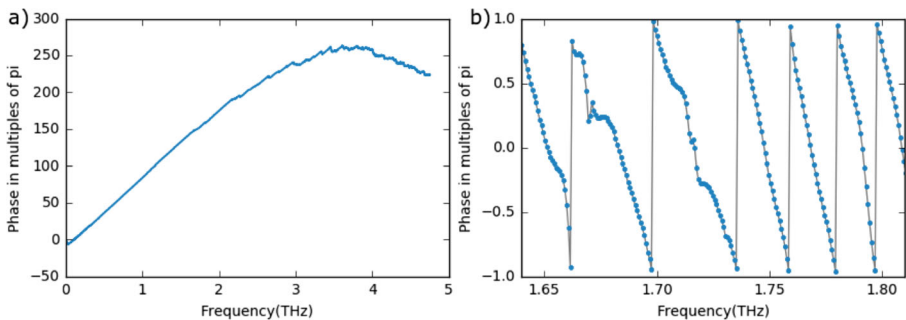


Fig. 3 **a** Unwrapped phase spectrum $\phi_{\text{meas}}(f_{\text{THz}})$ obtained with an integration time of 7 min. The slope is defined by the path length difference in the Tx and Rx path. Above 3 THz, the phase is dominated by noise. **b** Wrapped phase spectrum $\phi_{\text{meas}}(f_{\text{THz}})$ of a frequency subset showing the linear slope of $\phi_{\text{PLD}}(f_{\text{THz}})$ and its modification due to the water absorption lines at 1.66 THz, 1.67 THz, and 1.72 THz (see Eq. 4)

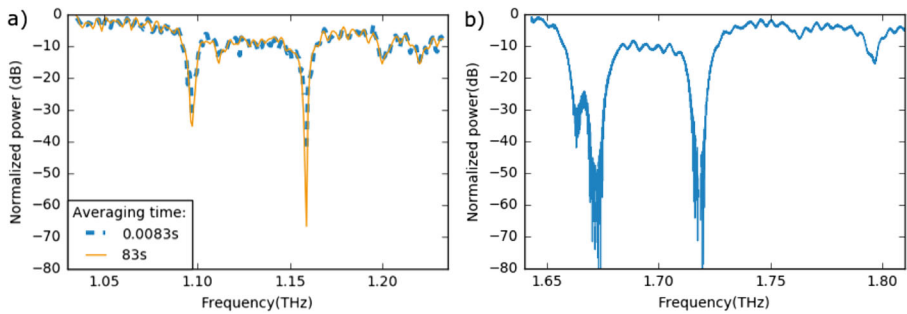


Fig. 4 **a** Normalized spectral power showing the prominent water absorption lines at 1.1 THz and 1.16 THz obtained at a continuous update rate of 120 Hz. The graph shows a single-shot measurement and averaging of 100 and 10,000 spectra. In this case, averaging is performed on the amplitude only and is subsequently corrected for the background (not shown), which has been recorded with a deactivated THz emitter. **b** Normalized spectral power presenting the high-frequency resolution mode using 20-MHz step size while reaching 40-MHz final resolution at 10-Hz continuous update rate. There were 10,000 spectra acquired and averaged in less than 20 min, the background is subtracted, and the data has been normalized. In both graphs, a) and b), the wiggles are attributed to interference within the silicon lens, which is used in emitter and receiver

5 Conclusion

An ultrafast cw THz spectrometer is presented showing homodyne acquisition of broadband cw THz spectra with high update rate. To the best of our knowledge, this is the first demonstration of a cw THz system featuring more than 2-THz bandwidth with a continuous update rate of 24 Hz. With averaging, more than 100-dB peak dynamic range and a bandwidth of more than 3.5 THz can be reached within 7 min. This demonstrates the good system term stability and proves the performance of the acquisition scheme. For a 300-GHz wide subset, the continuous update rate can reach even 120 Hz. With this performance, cw THz systems become interesting for inline-measurements or imaging applications. For example, a raster scan with 100×128 pixels can be performed in 7 min or 1.5 min with a 2-THz and 0.3-THz bandwidth, respectively. The presented system is very versatile, as it features high dynamic range, high resolution, and high bandwidth in combination with phase-sensitive detection and real-time update rates. Therefore, it can address many typical THz applications in non-destructive testing. Currently, the acquisition speed and update rate is mainly limited by the sampling speed of the data acquisition. Further optimizations will allow doubling of the update rate. In combination with task adopted sweep ranges and step size, layer thickness measurements with more than 100 Hz update rate are feasible. In the future, it comes in handy that optoelectronic cw THz systems are insensitive to dispersion in the optical domain, which makes it extremely attractive for photonic integration. By using well-established photonic building blocks from the telecom technology, i.e., lasers, phase modulators, optical amplifiers as well as passive components based on optical waveguide, compact or even handheld and low-cost THz spectroscopy systems can be realized. The system presented in this paper is a huge step forward to fast and integrated THz sensing devices.

Acknowledgments Portions of this work were presented at the 43rd International Conference on Infrared, Millimeter, and Terahertz Waves (IRMMW-THz) in 2018.

Open Access This article is distributed under the terms of the Creative Commons Attribution 4.0 International License (<http://creativecommons.org/licenses/by/4.0/>), which permits unrestricted use, distribution, and reproduction in any medium, provided you give appropriate credit to the original author(s) and the source, provide a link to the Creative Commons license, and indicate if changes were made.

Publisher's Note Springer Nature remains neutral with regard to jurisdictional claims in published maps and institutional affiliations.

References

1. J. L. M. Van Mechelen, "Dynamics of the stratification process in drying colloidal dispersions studied by terahertz time-domain spectroscopy," *Langmuir*, vol. 30, no. 43, pp. 12748–12754, 2014.
2. S. Krimi, J. Klier, J. Jonuscheit, G. Von Freymann, R. Urbansky, and R. Beigang, "Highly accurate thickness measurement of multi-layered automotive paints using terahertz technology," *Appl. Phys. Lett.*, vol. 109, no. 2, 2016.
3. I. S. Gregory, R. K. May, K. Su, and J. A. Zeitler, "Terahertz car paint thickness sensor: Out of the lab and into the factory," *Int. Conf. Infrared, Millimeter, Terahertz Waves, IRMMW-THz*, pp. 1–1, 2014.
4. J. Hauck, D. Stich, P. Heidemeyer, M. Bastian, and T. Hochrein, "Terahertz inline wall thickness monitoring system for plastic pipe extrusion," *AIP Conf. Proc.*, vol. 1593, no. 2014, pp. 86–89, 2014.
5. N. Vieweg, F. Rettich, A. Deninger, H. Roehle, R. Dietz, T. Göbel, and M. Schell, "Terahertz-time domain spectrometer with 90 dB peak dynamic range," *J. Infrared, Millimeter, Terahertz Waves*, vol. 35, no. 10, pp. 823–832, 2014.
6. R. J. B. Dietz, N. Vieweg, T. Puppe, A. Zach, B. Globisch, T. Göbel, P. Leisching, and M. Schell, "All fiber-coupled THz-TDS system with kHz measurement rate based on electronically controlled optical sampling," *Opt. Lett.*, vol. 39, no. 22, pp. 6482–6485, 2014.
7. T. Yasui, E. Saneyoshi, and T. Araki, "Asynchronous optical sampling terahertz time-domain spectroscopy for ultrahigh spectral resolution and rapid data acquisition," *Appl. Phys. Lett.*, vol. 87, no. 6, pp. 2–5, 2005.
8. R. Wilk, T. Hochrein, M. Koch, M. Mei, and R. Holzwarth, "OSCAT: Novel technique for time-resolved experiments without moveable optical delay lines," *J. Infrared, Millimeter, Terahertz Waves*, vol. 32, no. 5, pp. 596–602, 2011.
9. C. Hepp, S. Lüttjohann, A. Roggenbuck, A. Deninger, S. Nellen, T. Göbel, M. Jörger, and R. Harig, "A cw-terahertz gas analysis system with ppm detection limits," *Int. Conf. Infrared, Millimeter, Terahertz Waves, IRMMW-THz*, pp. 1–2, 2016.
10. D. Stanze, B. Globisch, R. Dietz, H. Roehle, T. Göbel, and M. Schell, "Multilayer Thickness Determination Using Continuous Wave THz Spectroscopy," *IEEE Trans. Terahertz Sci. Technol.*, vol. 4, no. 6, pp. 696–701, 2014.
11. D. Stanze, A. Deninger, A. Roggenbuck, S. Schindler, M. Schlak, and B. Sartorius, "Compact cw terahertz spectrometer pumped at 1.5 μm wavelength," *J. Infrared, Millimeter, Terahertz Waves*, vol. 32, no. 2, pp. 225–232, 2011.
12. D. De Felipe *et al.*, "Hybrid polymer / InP dual DBR laser for 1.5 μm continuous-wave Terahertz systems," *Proc. SPIE*, vol. 9747, pp. 1–7, 2016.
13. B. Sartorius, D. Stanze, T. Göbel, D. Schmidt, and M. Schell, "Continuous wave terahertz systems based on 1.5 μm telecom technologies," *J. Infrared, Millimeter, Terahertz Waves*, vol. 33, no. 4, pp. 405–417, 2012.
14. H.-C. Ryu, N. Kim, S.-P. Han, H. Ko, J.-W. Park, K. Moon, and K. H. Park, "Simple and cost-effective thickness measurement terahertz system based on a compact 155 μm $\lambda/4$ phase-shifted dual-mode laser," *Opt. Express*, vol. 20, no. 23, p. 25990, 2012.
15. K. H. Park *et al.*, "Photonic devices for tunable continuous-wave terahertz generation and detection," *Proc. SPIE*, vol. 7601, p. 898506, 2014.
16. D. S. Yee, J. S. Yahng, C. S. Park, H. D. Lee, and C. S. Kim, "High-speed broadband frequency sweep of continuous-wave terahertz radiation," *Opt. Express*, vol. 23, no. 11, pp. 14806–14814, 2015.
17. D. Stanze, T. Göbel, R. J. B. Dietz, B. Sartorius, and M. Schell, "High-speed coherent CW terahertz spectrometer," *Electron. Lett.*, vol. 47, no. 23, 2011.
18. J.-O. Wesstrom, G. Sarlet, S. Hammerfeldt, L. Lundqvist, P. Szabo, and P.-J. Rigole, "State-of-the-art performance of widely tunable modulated grating Y-branch lasers," *Opt. Fiber Commun. Conf. 2004. OFC 2004*, vol. 1, p. 389, 2004.
19. S. Preu, G. H. Döhler, S. Malzer, L. J. Wang, and A. C. Gossard, "Tunable, continuous-wave Terahertz photomixer sources and applications," *J. Appl. Phys.*, vol. 109, no. 061301, 2011.

20. T. Göbel, D. Stanze, B. Globisch, R. J. B. Dietz, H. Roehle, and M. Schell, “Telecom technology based continuous wave terahertz photomixing system with 105 decibel signal-to-noise ratio and 3.5 terahertz bandwidth,” *Opt. Lett.*, vol. 38, no. 20, pp. 4197–4199, 2013.
21. D. Stanze, H.-G. Bach, R. Kunkel, D. Schmidt, H. Roehle, M. Schlak, M. Schell, Martin, and B. Sartorius, “Coherent CW Terahertz System Employing Photodiode Emitters,” *Int. Conf. Infrared, Millimeter, Terahertz Waves, IRMMW-THz*, 2009.

Affiliations

Lars Liebermeister¹ · Simon Nellen¹ · Robert Kohlhaas¹ · Steffen Breuer¹ · Martin Schell¹ · Björn Globisch¹

Simon Nellen
simon.nellen@hhi.fraunhofer.de

Robert Kohlhaas
robert.kohlhaas@hhi.fraunhofer.de

Steffen Breuer
steffen.breuer@hhi.fraunhofer.de

Martin Schell
martin.schell@hhi.fraunhofer.de

Björn Globisch
bjoern.globisch@hhi.fraunhofer.de

¹ Fraunhofer Institute for Telecommunications, Heinrich Hertz Institute, HHI, Einsteinufer 37, 10587 Berlin, Germany